Electrocatalytic Hydrogenation of CO_2 to Hydrocarbons on Gold Catalyst in the Presence of Ionic Liquid

Arshid M. Ali[1]*, Aqeel Taimoor[1], Ayyaz Muhammad[1,2], Muhammad A. Daous[1] and Usman Saeed[1]
[1]*Department of Chemical and Materials Engineering, Faculty of Engineering, King Abdulaziz University, P.O. Box 80204, Jeddah 21589, Kingdom of Saudi Arabia.*
[2]*Institute of Chemical Engineering & Technology, University of the Punjab, Lahore, Pakistan.*
amsali@kau.edu.sa*

(Received on 14th January 2021, accepted in revised form 15th June 2021)

Summary: This study is aimed to investigate the electro-catalytic activity of Au supported on both CeO_2 and activated carbon (AC) to convert CO_2 to mixture of C_1-C_4 hydrocarbons in the presence of ionic liquid (IL) 1-butyl-3-methylimidazolium methylsulfonate. The studied catalyst samples were prepared by using simultaneous wet impregnation method. The sample containing 0.6 % Au showed higher electro-catalytic activity than the sample contained 0.3 % Au. Both, the average Au particles size and the transformation of layered non-uniformed semi-oval structure to flaked tiny circular like-structure were mainly responsible for the higher catalytic activity of 0.6Au-CeO_2-AC sample. In addition, the overall electro-catalytic activity depends upon the applied reaction voltage. Overall, the presence of IL, the surface morphology, and average Au particles size had played a key role in the electro-catalytic conversion of CO_2 to hydrocarbons.

Keywords: Electro-Catalysis, Gold catalyst, Cerium Oxide, Activated Carbon, Electro-catalytic Activity.

Introduction

The global warming, resulted from the massive release of CO_2 and other greenhouse gases due to industrial activities and intensive fossil fuel utilization, is a serious threat to both environmental and ecological balance on our planet. Reported global annual average increase of atmospheric CO_2 concentration is 2.54 ppm, which is yet very high comparing to existing stringent environmental quality standards [1].

Various methods for utilization of CO_2 emissions like an artificial photosynthesis [2, 3], photocatalysis [4-6] and electrolysis [7, 8] had been proposed. They are applied with certain level of success; however, none of the reported methods is economically viable because either it requires very high current density, high photon energy and/or very high temperature to overcome the thermodynamic behavior CO_2.

Among possible pathways for the abatement of the CO_2, is to hydrogenate it to value added liquid hydrocarbon mixtures, which can be used as a motor fuel.

In the recent past, many studies [9-11] had used IL for the carbon capture technologies. The reasons for this tendency are the unique properties of IL compared to traditional solvents. These include negligible vapor pressure, high thermal and chemical stability, selective and high solubility capacity and good recyclability [9]. Because of thermodynamically stable nature of CO_2 [4], it requires a lot of reaction energy to activate CO_2 and facilitate CO_2 conversion to liquid hydrocarbon fuels.

Recently, many researchers have focused to study electrocatalytic methods for conversion of CO_2 into harmless and useful hydrocarbon fuels [12-23].

As per author's best knowledge, no study was reported using combination of both electrochemical and catalytic methods for CO_2 abatement. The novelty of this work is the use combination of both catalytic and electro catalytic methods, in the presence of ionic liquid. The electro-chemical redox reactions are facilitated by the electro-catalytic method via decreasing of the activation energy (voltage applied *i.e.,* CO_2 overpotential). This is an important approach to facilitate CO_2 conversion to useful products.

The electrochemical bath may or may not be aqueous. As CO_2 is sparingly soluble in water. Therefore, the other electrochemically active solvents like ionic liquid (such as 1-butyl-3-methylimidazolium methanesulfonate) might be used in the presence of catalysts (in our case gold supported on activated carbon and ceria).

Experimental

Catalyst Preparation

The studied samples were prepared by using simultaneous wet impregnation technique [24-26].

*To whom all correspondence should be addressed.

Precise amount of each component of the catalyst recipe were obtained from freshly prepared stocks solutions. All the stock solutions were prepared by using the deionized water (DIW). Well mixed Au salt solution was added to the dried powder mixture composed of cerium oxide and activated carbon (AC) in a Rotavapor flask at 60 °C. After 4 h of wet impregnation, a vacuum was applied to obtained semi-dry paste. Next, the grinded powder was dried at120 °C for 5 h and calcined at 450 °C for an overnight. The dried and calcined powder was pelletized by using laboratory palletizer. Two different Au loadings 0.3% wt and 0.6% wt were used to obtained 0.3Au-CeO_2-AC and 0.6Au-CeO_2-AC samples.

Activity Tests

The catalytic activity of 0.3Au-CeO_2-AC and 0.6Au-CeO_2-AC samples were tested in a three-electrode system coupled with PG STAT-101 potentiostat (AUTOLAB) equipped with NOVA software. Ag/AgCl electrode was used as standard electrode and a platinum electrode was used as counter electrode (Fig. 1). A graphite electrode was used as a working electrode for the electro-catalytic reaction. A temperature probe was used to monitor the reaction temperature, immersed in oil circulation in the cell jacket. All the experiments were performed under atmospheric pressure. Pure carbon dioxide was bubbled through the solution continuously at a constant flow rate of 1 $cm^3.min^{-1}$. Before starting the reaction, the electrodes were immersed in the IL and left for 30 mins to achieve a steady state. The reaction products were monitored by using as gas chromatogram (SRI 8610C, USA) equipped with both FID and TCD detectors. A TG-BOND Alumina KCl column under highly pure N_2 flow was used to analyse reaction products.

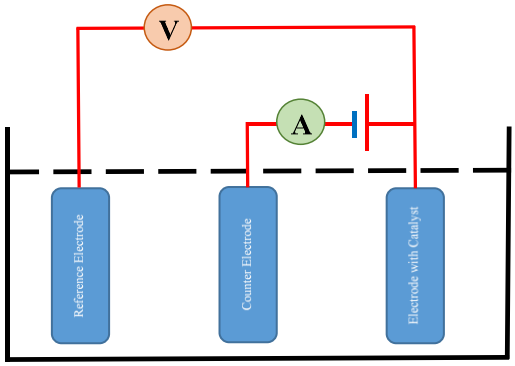

Fig 1: Schematic of three electrode system, for electrochemical reaction.

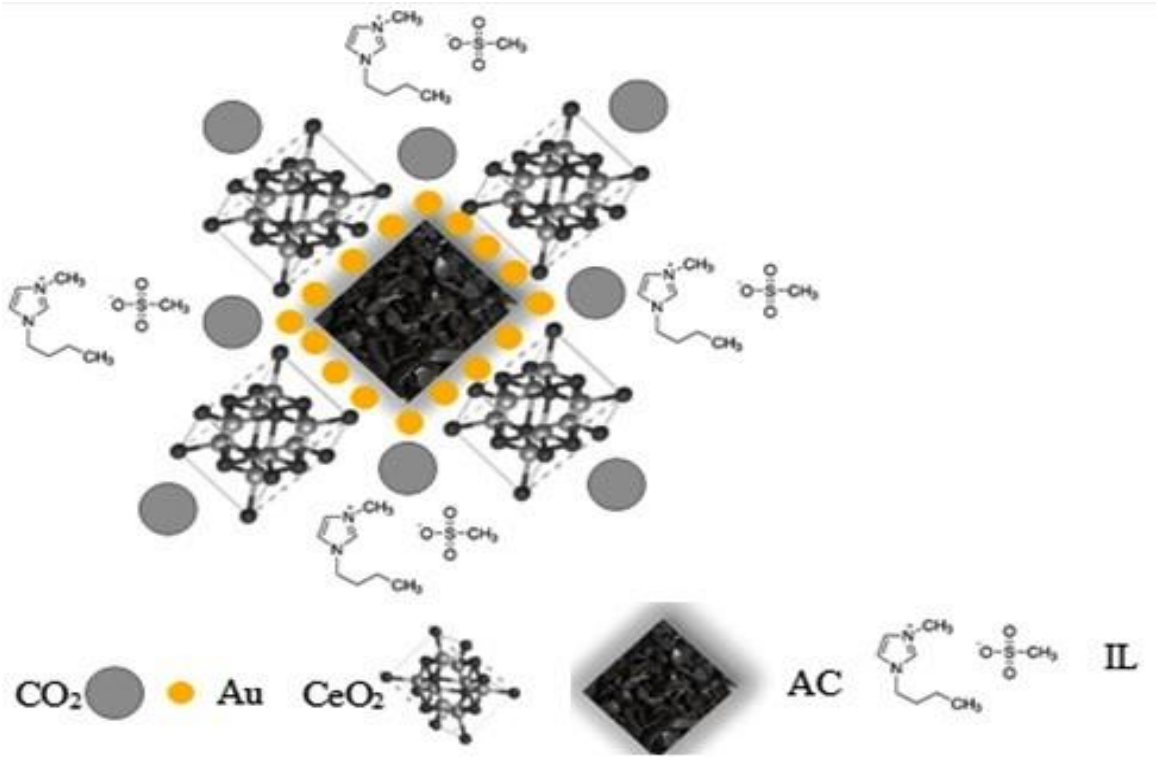

Fig. 2: Suggested mechanism of CO_2 conversion to hydrocarbons in IL.

Catalyst Characterization

STA 449 F3 simultaneous TG-DSC was used to analyze the catalyst's thermal stability, phase transition and decomposition behavior. A precise amount of grounded powder sample was placed in a DSC/TG alumina crucible. The temperature programme was set from 20 to 900 ºC with a different temperature step size under either air and/or nitrogen flow of 10 cm^3 min^{-1}. The morphology micrograms were obtained by using field emission scanning electron microscope (FESEM) from JEOL-JSM 7600F and TEM. A conductive carbon tape was used to place the sample to specimen stub. Before FESEM, all the samples were sputtered with platinum by using auto fine coater (JFC-1600, JEOL-JSM 7600F) for 30 s under 30mA and 3.5 Nm^{-2}. The detailed FESEM was performed at 5 kV with WD of 7.6 mm.

Results and Discussions

The catalytic activity of studied samples is shown in Figs. 3a-e and Table-1. The catalytic activities of both the samples were measured in terms of total C_1-C_4 hydrocarbons produced, the amount of CO produced, and remaining reaction products (termed as others).

The % conversion of CO_2 and C_1-C_4 hydrocarbons % selectivity was calculated by using following equations:

$$\%\ Conversion = \frac{unreacted\ Moles\ of\ CO_2}{Moles\ of\ CO_2\ in\ feed} \times 100$$

$$\%\ Selectivity = \frac{Moles\ of\ desired\ product}{Moles\ of\ undesired\ product} \times 100$$

In case of 0.3Au-CeO_2-AC sample, the overall conversion of CO_2 to C_1-C_4 hydrocarbons was 6.8%. In addition to C_1-C_4 hydrocarbons, a significant amount of CO was also produced during the catalytic reaction. The selectivity of C_1-C_4, CO and others were 58.40 %, 22.60% and 19.40% respectively. Whereas, in case of the 0.6Au-CeO_2-AC the sample, the overall conversion of CO_2 to C_1-C_4 hydrocarbons was 13.5%. Also, the 0.6Au-CeO_2-AC sample had shown reduced formation of CO during the reaction. The selectivity of C_1-C_4, CO and others were 60.45 %, 6.70% and 32.85 % respectively. The sample without containing Au, almost show negligible conversion. The presence of sulfonyl and sulphonic acid group in the same ionic liquid is mainly responsible for influencing/enhancing the catalytic activity with better yield of desired products.

In comparison, the 0.6Au-CeO_2-AC sample had shown an overall higher conversion of CO_2 to hydrocarbons as to 0.3Au-CeO_2-AC sample. Also, the 0.6Au-CeO_2-AC catalyst had shown least formation of CO during the reaction as to 0.3Au-CeO_2-AC sample. However, in case of 0.6Au-CeO_2-AC sample, the selectivity of others was higher as to 0.3Au-CeO_2-AC sample. This could be because of the smaller Au particle size (see the Table 1) as well as favorable impact of the ionic liquid interaction with either Au, CeO_2 and AC.

To study the effect of the operational voltage to the catalytic activity, the best performed catalyst (in terms of % conversion), the 0.6Au-CeO_2-AC sample were tested under different electrode potentials.

The results showed that with gradual increase in operational voltage, up to 0.35 V, a slight increase in overall conversion was observed. However, beyond 0.35 V no further increase was observed, and the overall catalytic activity remained unchanged up to 0.40 V. This showed an optimal operational voltage is essential and favorable.

The faradaic efficiency (FE) vs applied voltage results is shown in Fig. 3b. For both 0.3Au-CeO_2-AC and 0.6Au-CeO_2-AC 0.6, the FE remained almost constant and stable in the voltage range of 0.32 V to 0.37 V. The average FE in this voltage range for both 0.6Au-CeO_2-AC and 0.3Au-CeO_2-AC catalysts was 75% and 27.5% respectively. The value of FE, in the voltage range of 0.32 V to 0.37 V, conforms to both conversion of CO_2 and C_1-C_4 hydrocarbons selectivity. In addition, based on linear sweep voltammetry (LSV) comparison (see Figs. 3c), the 0.6Au-CeO_2-AC catalyst had higher catalytic activity as to 0.3Au-CeO_2-AC catalyst under similar reaction conditions.

Table-1: Summary of the Catalytic Activity Tests.

Catalyst	CO_2 % Conversion	%Selectivity			Particle Size (nm)		Sieve size (mm)
		C_1-C_4 Hydrocarbons	CO	Others	Au	CeO_2	AC
CeO_2-AC	~1.0	20.32	16.36	63.32	-	12.54	0.58
0.3Au-CeO_2-AC	6.8	58.30	22.60	19.10	4.90	12.54	0.58
0.6Au-CeO_2-AC	13.56	60.45	6.70	32.85	4.34	10.79	0.58

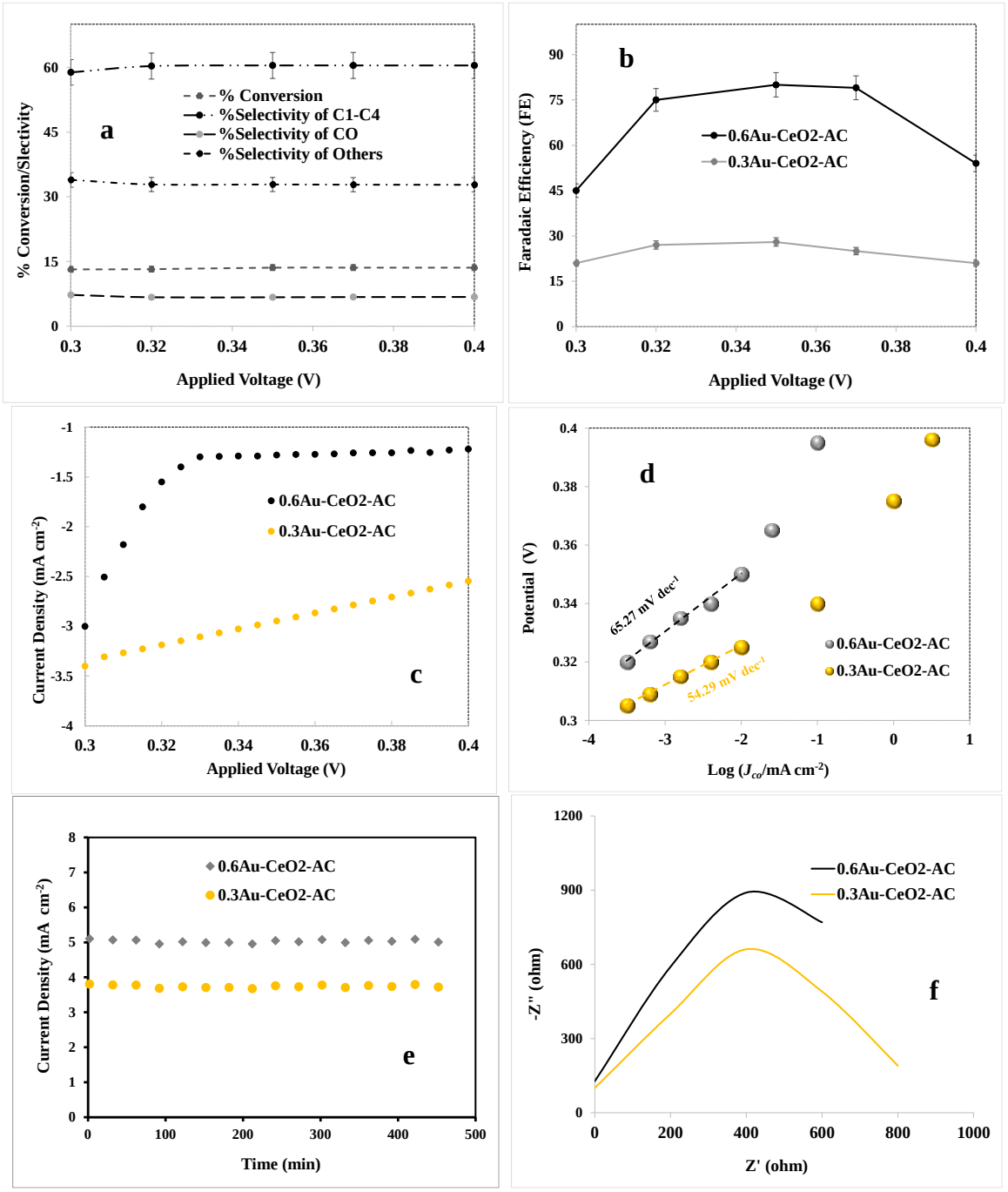

Fig 2: (a) Electrocatalytic activity of 0.3Au-CeO_2-AC and 0.6Au-CeO_2-AC samples; (b) The faradaic efficiency; (c) comparison of linear sweep voltammetry (LSV); (d) Tafel plots at different applied potential; (e) long-term durability test comparison of 0.3Au-CeO_2-AC and 0.6Au-CeO_2-AC samples and (f) impedance analysis.

To get an insight to kinetics, a Tafel slope was calculated, and results are shown in Fig. 3d. The Tafel's slope, an indication kinetics for CO formation, for both 0.6Au-CeO_2-AC and 0.3Au-CeO_2-AC catalysts were 65.27 mV dec^{-1} and 54.29 mV dec^{-1} respectively. The formation of C_1-C_4 hydrocarbons may be attributed to HCOO* intermediate at certain applied voltage range and presence of suitable ionic liquid [19, 27]. The high electron mobility (Fig. 3f) further enhanced the formation of favorable reaction species of C_1-C_4 hydrocarbons [28]. In addition, both 0.6Au-CeO_2-AC and 0.3Au-CeO_2-AC catalysts exhibited a very stable and consistent electrocatalytic activity for 7.5 hrs (see Fig. 3e). The stable and consistent activity is attributed to the ability of an ionic liquid can be re-used multiple times without jeopardizing the catalytic activity [29].

Table-1: Summary of the effect of the operational voltage to the catalytic activity of 0.6Au-CeO_2-AC.

Operating Voltage	% Conversion	%Selectivity		
		C_1-C_4 Hydrocarbons	CO	Others
0.30	**13.15**	**58.85**	**7.24**	**33.91**
0.32	**13.20**	**60.30**	**6.70**	**32.85**
0.35	**13.56**	**60.45**	**6.70**	**32.85**
0.37	**13.56**	**60.45**	**6.75**	**32.80**
0.40	**13.56**	**60.45**	**6.77**	**32.78**

To elucidate it further, a detailed surface morphology of both un-used and used samples were studied by using filed emission scanning electron microscopy (FESEM) and transmission electron microscopy (TEM). The results are shown in Figs. 4 and 6. Before the electrocatalytic reaction, the layered non-uniformed semi-oval morphology of 0.6Au-CeO_2-AC partially resemble to the similar morphology of 0.3Au-CeO_2-AC sample. The slight difference is attributed to the different amount of Au loadings. The FESEM results suggested that higher content of Au produced a clear and uniform morphology as to lower content of Au (see Figs. 4A and 4C).

After the electrocatalytic reaction, layered non-uniformed semi-oval morphology significantly changed to flaked tiny circular like-structure (Figs.4A-B and Figs.4C-D). This change in 0.6Au-CeO_2-AC sample was more prominent as to 0.3Au-CeO_2-AC sample. It clearly indicated that either the presence of ionic liquid and/or electrode potential has significantly changed the surface morphologies. Apparently, it helped in increasing the surface area. Because, flaked tiny circular like-structure has higher surface area as to layered semi-circular structure. In addition, the less change occurred in surface morphology of 0.3Au-CeO_2-AC as to 0.6Au-CeO_2-AC sample after the electrocatalytic reaction. It was also observed that Au particles were mostly present in the vicinity between AC and CeO_2 (Figs. 4 and 6).The higher overall conversion of 0.6Au-CeO_2-AC catalysts could be attributed to the increased available surface area of the layered non-uniformed semi-oval morphology during the electrocatalytic reaction. Due to an interfaced structure of the as-made hybrid system is also equally important for the significant catalytic activity of 0.6Au-CeO_2-AC and 0.3Au-CeO_2-AC catalysts. In addition, The change in morphology is attributed to the potential transition of crystal lattice due to the reduced/oxidizing species generated after the applied voltage [30]. In general, both nature of the morphology and available surface area during the electrocatalytic reaction played a key role to convert CO_2 to hydrocarbons.

In general, the enhanced the electro-catalytic activity of 0.6 Au-CeO_2-AC sample is attributed to:

i. Au and Ce particle size
ii. surface morphology
iii. Possible interacted states between Ce, Au and AC.

To encapsulate it further, simultaneous TG-DSC analysis of both electro-catalytically used and unused 0.3Au-CeO_2-AC and 0.6Au-CeO_2-AC samples were also studied. The results are shown in Figs. 5A-D. Simultaneous TG-DSC profiles of both un-used 0.3Au-CeO_2-AC and 0.6Au-CeO_2-AC sample almost resembles to each other. Almost, both un-used 0.3Au-CeO_2-AC and 0.6Au-CeO_2-AC samples exhibited similar morphologies composed of single semi-crystalline structure. In addition, both the 0.3Au-CeO_2-AC and 0.6Au-CeO_2-AC samples had shown two regions of glass transition at temperatures after 800 ºC, which is beyond the studied electrocatalytic reaction temperature range. So, both the samples remained stable (in terms of glass transition temperature) and there no formation polymeric products at these reaction temperatures.

However, after the reaction, the TG-DSC profiles of used 0.3Au-CeO_2-AC and 0.6Au-CeO_2-AC samples exhibited a significant change in surface morphologies [see Figs. 5A, 5C and Figs 5B, 5D] belonged to same crystal structure. This change in surface morphologies is attributed to the potential release of energy during the electrocatalytic reaction in the presence of ionic liquid. In addition, no polymeric product is formed on the surface of both used and un-used 0.3Au-CeO_2-AC and 0.6Au-CeO_2-AC samples. This finding clearly indicated that during the reaction at different applied voltage, both the surface morphology and apparent surface area did change, and this phenomenon played a key role in the overall electro-catalytic activity of both samples.

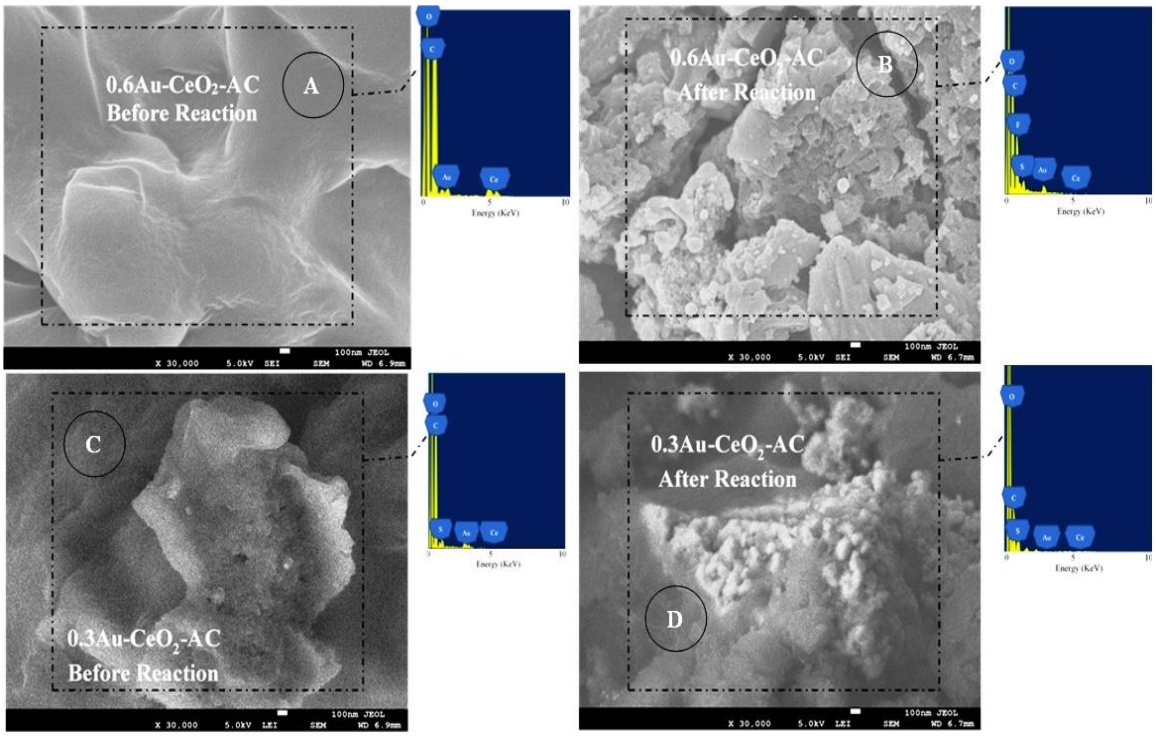

Fig. 4: FESEM analysis of 0.6Au-CeO_2-AC and 0.3Au-CeO_2-AC sample both before and after the electrocatalytic reaction.

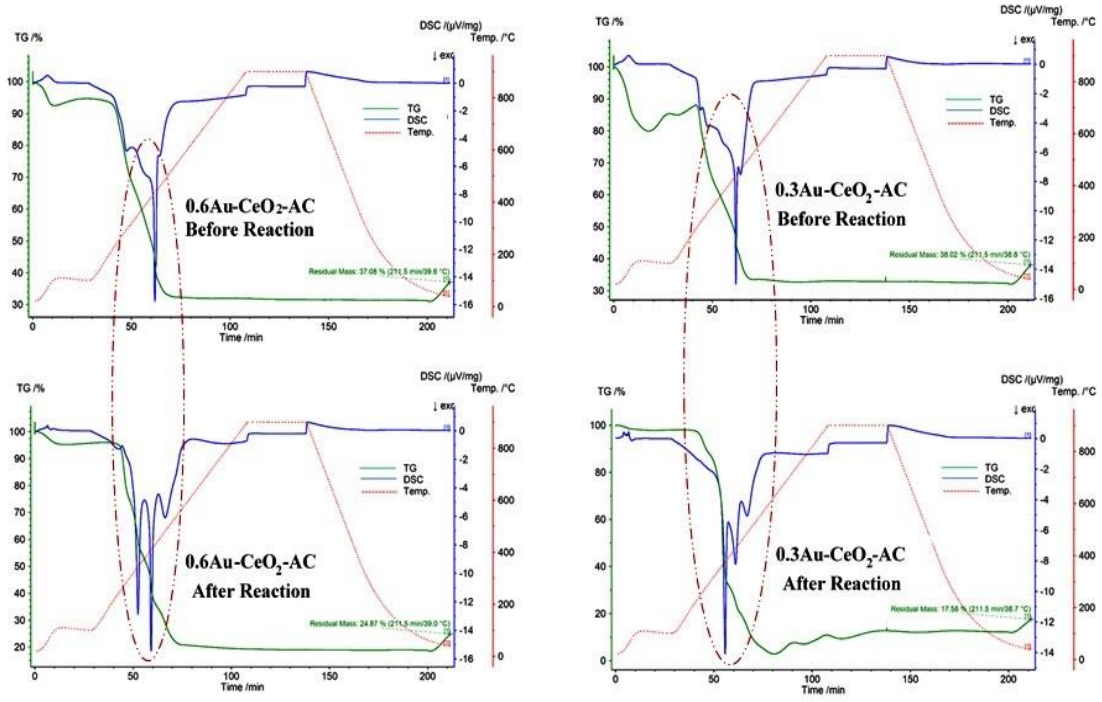

Fig 3: Simultaneous TG-DSC analysis of 0.6Au-CeO_2-AC and 0.3Au-CeO_2-AC both before and after the electrocatalytic reaction.

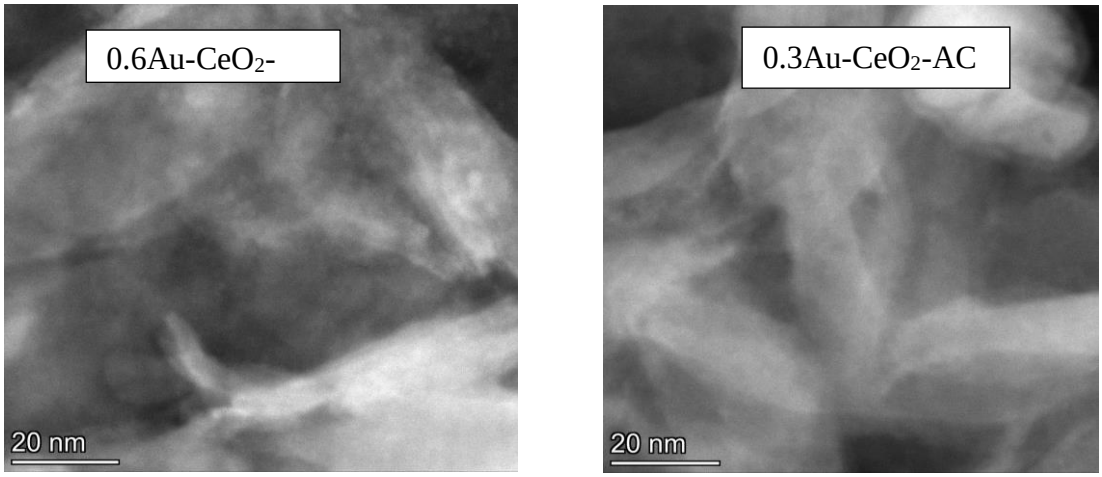

Fig 4: TEM analysis comparison of 0.6Au-CeO_2-AC and 0.3Au-CeO_2-AC.

Conclusions

In summary, 0.6Au-CeO_2-AC and 0.3Au-CeO_2-AC samples were prepared by using simultaneous wet impregnation method. The electro-catalytic activity for CO_2 conversion of both samples was measured, in the presence of ionic liquid, to hydrocarbon. The 0.6Au-CeO_2-AC sample had shown higher electro-catalytic activity. The higher electro-catalytic activity, attributed to the formed layered non-uniformed semi-oval morphology of support and smaller Au particle size of 4.34 nm. During the reaction, the formed layered non-uniformed semi-oval morphology was significantly changed to flaked tiny circular like-structures, which apparently increase the available surface area and easy accessibility of Au to initiate reaction. In addition, the overall electro-catalytic activity also depends upon the applied reaction voltage. Overall, the presence of ionic liquid, the surface morphology, and average Au particles size had played a key role in the electro-catalytic conversion of CO_2 to hydrocarbons.

Acknowledgements

This project t was funded by Saudi Arabian Basic Industries Corporation (SABIC) and the Deanship of Scientific Research (DSR), King Abdulaziz University, Jeddah, under grant No. (S-17-532-37). The authors, therefore, gratefully acknowledge with thanks to SABIC and DSR for technical and financial support.

References

1. J. G. J. Olivier.
2. B. Kumar, M. Llorente, J. Froehlich, T. Dang, A. Sathrum, C. P. Kubiak, Photochemical and Photoelectrochemical Reduction of CO2, Annual Review of Physical Chemistry, **63,** 541 (2012).
3. A. Jaworek, A. T. Sobczyk, Electrospraying route to nanotechnology: An overview, *Journal of Electrostatics*, **66**, 197 (2008).
4. S. K. Parayil, A. Razzaq, S.-M. Park, H. R. Kim, C. A. Grimes, S.-I. In, Photocatalytic conversion of CO2 to hydrocarbon fuel using carbon and nitrogen co-doped sodium titanate nanotubes, *Applied Catalysis A: General*, **498**, 205 (2015).
5. W. Tu, Y. Zhou, Z. Zou, Photocatalytic Conversion of CO2 into Renewable Hydrocarbon Fuels: State-of-the-Art Accomplishment, Challenges, and Prospects, *Advanced Materials*, **26**, 4607 (2014).
6. L. Yuan, Y.-J. Xu, Photocatalytic conversion of CO2 into value-added and renewable fuels, *Applied Surface Science*, **342**, 154 (2015).
7. H. Yin, X. Mao, D. Tang, W. Xiao, L. Xing, H. Zhu, D. Wang, D. R. Sadoway, Energy & *Environmental Science*, **6**, 1538 (2013).
8. S. Uhm, Y. D. Kim, Electrochemical conversion of carbon dioxide in a solid oxide electrolysis cell, *Current Applied Physics*, **14,** 672 (2014).
9. S. Mortazavi-Manesh, M. A. Satyro, R. A. Marriott, Screening ionic liquids as candidates for separation of acid gases: Solubility of hydrogen sulfide, methane, and ethane *AIChE Journal*, **59**, 2993 (2013).
10. R. Pauliukaite, A. P. Doherty, K. D. Murnaghan, C. M. A. Brett, Application of room temperature ionic liquids to the development of electrochemical lipase biosensing systems for

water-insoluble analytes, *Journal of Electroanalytical Chemistry*, **656**, 96 (2011).
11. H. Y. Xiong, T. Chen, X. H. Zhang, S. F. Wang, Electrochemical property and analysis application of biosensors in miscible nonaqueous media—Room-temperature ionic liquid *Electrochemistry Communications*, **9**, 1648 (2007).
12. B. P. Sullivan, in: B.P. Sullivan (Ed.) Electrochemical and Electrocatalytic Reactions of Carbon Dioxide, Elsevier, *Amsterdam*, 1993, pp. v.
13. W. Zhu, R. Michalsky, Ö. Metin, H. Lv, S. Guo, C. J. Wright, X. Sun, A. A. Peterson, S. Sun, Active and Selective Conversion of CO2 to CO on Ultrathin Au Nanowires, *Journal of the American Chemical Society*, **135**, 16833 (2013).
14. Q. Lu, J. Rosen, Y. Zhou, G. S. Hutchings, Y. C. Kimmel, J. G. Chen, F. Jiao, A selective and efficient electrocatalyst for carbon dioxide reduction, *Nat Commun*, 5 (2014).
15. C. Jia, K. Dastafkan, W. Ren, W. Yang, C. Zhao, Carbon-based catalysts for electrochemical CO2 reduction, *Sustainable Energy & Fuel*s, **3** 2890 (2019).
16. Y. Hori, in: C.G. Vayenas, R.E. White, M.E. Gamboa-Aldeco (Eds.) Modern Aspects of Electrochemistry, Springer New York, New York, NY, 2008, pp. 89.
17. X. L. Senlin Chu, Alex W. Robertson, Zhenyu Sun, Electrocatalytic CO2 Reduction to Ethylene over CeO2-Supported Cu Nanoparticles: Effect of Exposed Facets of CeO_2, *Acta Phys. -Chim. Sin.*, **37**, 2009023 (2021).
18. S. Chu, X. Yan, C. Choi, S. Hong, A. W. Robertson, J. Masa, B. Han, Y. Jung, Z. Sun, Stabilization of Cu+ by tuning a CuO–CeO2 interface for selective electrochemical CO2 reduction to ethylene, *Green Chemistry*, **22** 6540 (2020).
19. Z. Han, C. Choi, H. Tao, Q. Fan, Y. Gao, S. Liu, A. W. Robertson, S. Hong, Y. Jung, Z. Sun, Tuning the Pd-catalyzed electroreduction of CO_2 to CO with reduced overpotential, *Catalysis Science & Technology*, **8** 3894 (2018).
20. R. Calmanti, M. Selva, A. Perosa, Tungstate ionic liquids as catalysts for CO_2 fixation into epoxides, *Molecular Catalysis*, **486**, 110854 (2020).
21. N. Yao, C. Chen, D. J. Li, Y. L. Hu, Benzotriazolium Ionic Liquid Immobilized on Periodic Mesoporous Organosilica as an Effective Reusable Catalyst for Chemical Fixation of C[O.sub.2] into Cyclic Carbonates, *Journal of Environmental Chemical Engineering*, **8** 103953 (2020).
22. P. Zhang, Y. Jin, Z. Jiang, G. Xie, Q. Zhang, X. Li, Gas-phase dehydrochlorination of 1, 1, 2, 2-tetrachloroethane over the non-metal supported ionic liquid catalyst, *Chinese Journal of Chemical Engineering*, **28** 1623 (2020).
23. K. Zuraiqi, A. Zavabeti, F.-M. Allioux, J. Tang, C. K. Nguyen, P. Tafazolymotie, M. Mayyas, A. V. Ramarao, M. Spencer, K. Shah, C. F. McConville, K. Kalantar-Zadeh, K. Chiang, T. Daeneke, Liquid Metals in Catalysis for Energy Applications, *Joule*, **4**, 2290 (2020).
24. Y. Alhamed, M. Umar, M. Daous, A. A. Al-Zahrani, L. Petrov, *Comptes rendus de l'Acade'mie bulgare des Sciences*, **66** 997 (2013).
25. A. M. Ali, M. A. Daous, A. A. M. Khamis, H. Driss, R. Burch, L. A. Petrov, Strong synergism between gold and manganese in an Au–Mn/triple-oxide-support (TOS) oxidation catalyst, *Applied Catalysis A: General*, **489,** 24 (2015).
26. A. M. Ali, M. A. Daous, A. Arafat, A. A. AlZahrani, Y. Alhamed, A. Tuerdimaimaiti, L. A. Petrov, Effect of Au precursor and support on the catalytic activity of the nano-Au-catalysts for propane complete oxidation, *Journal of Nanomaterials*, **2015** 10 (2015).
27. H. Tao, X. Sun, S. Back, Z. Han, Q. Zhu, Alex W. Robertson, T. Ma, Q. Fan, B. Han, Y. Jung, Z. Sun, Doping palladium with tellurium for the highly selective electrocatalytic reduction of aqueous CO_2 to CO, *Chemical Science*, **9,** 483 (2018).
28. Y. Zhao, X. Jia, G. Chen, L. Shang, G. I. N. Waterhouse, L.-Z. Wu, C.-H. Tung, D. O'Hare, T. Zhang, Ultrafine NiO Nanosheets Stabilized by TiO2 from Monolayer NiTi-LDH Precursors: An Active Water Oxidation Electrocatalyst, *Journal of the American Chemical Society*, **138** 6517 (2016).
29. R. Ratti, Ionic Liquids: Synthesis and Applications in Catalysis, *Advances in Chemistry*, **2014**, 729842 (2014).
30. M. Okido, K. Nishikawa, K. Kuroda, R. Ichino, Z. Zhao, O. Takai, Evaluation of the Hydroxyapatite Film Coating on Titanium Cathode by QCM *Materials transactions*, **43** 3010 (2002).